Structure and composition of the Trinil femora: Functional and taxonomic implications

Russell Ciochon, Justin Sipla

Journal of Human Evolution

Structure and composition of the Trinil femora: Functional and taxonomic implications

Christopher B. Ruff [a,*], Laurent Puymerail [b,c], Roberto Macchiarelli [c,d], Justin Sipla [e], Russell L. Ciochon [f]

[a] Center for Functional Anatomy and Evolution, Johns Hopkins University School of Medicine, 1830 E. Monument St., Baltimore, MD 21111, USA
[b] Unité d'Anthropologie bio-culturelle, Droit, Éthique et Santé (ADÉS), UMR 7268, Université d'Aix-Marseille-EFS-CNRS, Marseille, France
[c] Département de Préhistoire, MNHN, UMR 7194, Paris, France
[d] Département Géosciences, Université de Poitiers, France
[e] Department of Anatomy and Cell Biology, University of Iowa, Iowa City, IA 52242, USA
[f] Department of Anthropology and Museum of Natural History, University of Iowa, Iowa City, IA 52242, USA

ABSTRACT

The original hominin femur (Femur I) and calotte discovered at Trinil, Java by Eugene Dubois in 1891/1892 played a key role in the early history of human paleontology by purportedly demonstrating the contemporaneity of archaic cranial form with modern human erect (bipedal) posture. On this basis, both specimens were subsequently assigned to *Pithecanthropus erectus*, later transferred to *Homo erectus*. However, chronological and phylogenetic links between the two have been questioned from the beginning. Four additional hominin partial femora (Femora II–V) from Trinil were subsequently described but have played a relatively minor part in evolutionary scenarios. Here we present the results of a new analysis of structural and density characteristics of the Trinil femora obtained using computed tomography. Trinil Femur I shows none of the characteristics typical of early *Homo* femora from elsewhere in Asia or Africa, including a relatively long neck, increased mediolateral bending rigidity of the mid-proximal shaft, or a low position of minimum mediolateral breath on the shaft. In contrast, Femora II–V all demonstrate features that are more consistent with this pattern. In addition, material density distributions within the specimens imply more recent and less complete fossilization of Femur I than Femora II–V. Thus, it is very likely that Trinil Femur I derives from a much more recent time period than the calotte, while the less famous and less complete Femora II–V may represent *H. erectus* at Trinil. The morphological variation within the Trinil femora can be attributed to broader changes in pelvic morphology occurring within the *Homo* lineage between the Early and late Middle Pleistocene.

© 2015 Published by Elsevier Ltd.

Introduction

The discovery by Eugene Dubois in 1891/2 of a fossilized hominin calotte and femur (and two molars) from the site of Trinil next to the Solo River, Java was one of the most significant events in the history of human paleontology. The calotte was markedly more primitive than any other hominin fossil found to date—Dubois himself originally considered it to be more closely related to chimpanzees and only later assigned it to the human lineage (Dubois, 1894), a viewpoint that was initially questioned by a number of scientists but eventually widely accepted (Theunissen, 1989; de Vos, 2008). In contrast, the femur was remarkably similar to those of modern humans (see Fig. 1). It was also remarkable for the large exostosis on its proximal shaft, which has been given various explanations (see Discussion). Its overall similarity to modern humans was immediately recognized by Dubois, who noted its length and relative slenderness (indicating a long lower limb relative to body weight), bicondylar angle, and other human-like features, concluding that "It follows with complete certainty from this examination of the thigh bone that the Javanese *Anthropopithecus* stood and walked in the same upright position as man" (Dubois, 1893, p. 13). On this basis he assigned the species name *erectus* to both the calotte and femur, later transferring them to *Pithecanthropus erectus* (Dubois, 1894), which 50 years afterwards was subsumed into *Homo erectus* (Mayr, 1944, 1950).

Figure 1. Anterior photographs of the original Trinil Femora I–V specimens. Femora I, III, and V are left sides, and Femora II and IV are right sides. Femora I and II are shown oriented in approximate anatomical position, while the others are oriented with the shaft positioned vertically.

However, from the outset questions were raised regarding the association between the calotte and femur. Dubois did not carry out the excavations himself and was not present at the site when the calotte and femur were discovered (nine months apart; Shipman, 2001). He included no stratigraphic diagrams or site maps in his initial publications (Dubois, 1893, 1894), only producing these in later presentations (Dubois, 1895, 1896). He argued from the beginning, however, that the calotte and femur were found at the same level or layer in the site, although some 15 m apart (later amended to 10–12 m; Dubois, 1932). However, on the basis of other contemporary documentary evidence, Bartsiokas and Day (1993) questioned the attribution of the two specimens to the same stratum, noting that because of a downward inclination of lower beds in the site, the femur, although at the same absolute level relative to the river, may have come from a stratigraphically more recent layer. The later demonstration of much more recent (Late Pleistocene) deposits at the Trinil site (Barstra, 1982), along with other chemical evidence (see below), also lent weight to the viewpoint that the original Trinil femur derived from a later time period than the calotte.

The very modern morphology of the femur—more modern than other hominin fossils known at the time (i.e., European Neandertal specimens)—also raised questions about its antiquity (Cunningham, 1895; Pearson and Bell, 1919). Dubois seems to have anticipated this issue and took pains to point out several features that, while not changing his overall functional interpretation, purportedly distinguished the femur from those of modern humans, including in particular a more convex popliteal surface (Dubois, 1894, 1896, 1926). His statement at a meeting in 1895 reflects this potential conflict: "It [the femur] has a *human character* … but that does not mean that it is a *human femur*" (italics original; Dubois, 1895: 159). However, other researchers demonstrated that these features could in fact commonly be found among modern humans (Hepburn, 1896; Pearson and Bell, 1919).

The discovery of the Zhoukoudian femora, associated with crania similar to the Trinil calotte but showing a different morphology, also called into question the age and association of the Trinil femur

(Weidenreich, 1938). Weidenreich described several characteristics of the Zhoukoudian femora that together set them apart from those of modern humans, including marked mediolateral (M-L) widening of the shaft (platymeria), a distal position of minimum M-L breadth (well below midshaft), and thick cortices. None of these features characterized the Trinil femur, leading him to conclude that the femur was most likely "one of recent man and with no close relationship to the skull cap" (Weidenreich, 1938: 615; see also von Koenigswald and Weidenreich, 1939). Le Gros Clark (1939) questioned this assertion, arguing that the features described by Weidenreich for the Zhoukoudian femora represented variable and developmentally plastic features (basing this in part on the comparative studies of Buxton [1938]). However, Weidenreich defended his position with more detailed analyses of both the Zhoukoudian and Trinil specimens (Weidenreich, 1941). Day (1971) extended these comparisons to the (African) *H. erectus* OH 28 femur, which exhibited many of the same features as the Zhoukoudian femora, and again called into question the age and taxonomic status of the Trinil femur. He later incorporated these features into a "femoropelvic complex" that characterized Early and early Middle Pleistocene *Homo* specimens from East Africa, Europe, and Asia (but not the original Trinil femur; Day, 1984, 1986a). The more recently discovered late Early Pleistocene femora from Bouri, Ethiopia, also fit this pattern (Gilbert, 2008).

In a series of papers in the 1930s, Dubois described five other partial femora excavated at Trinil in 1900 and discovered in collections of the Leiden Museum (Dubois, 1932, 1934, 1935). The sixth femoral specimen may not be hominin and is not from the Trinil locality (Day and Molleson, 1973), so is not further considered here. The others, referred to as Femora II, III, IV, and V, are shown in Figure 1 along with the original Femur I. None is complete, although Femur II preserves much of the neck as well as shaft, and Femora III and IV preserve most of the shaft, while Femur V is more fragmentary. All are also more weathered than Femur I. Their stratigraphic provenience is not certain, although they came out of the collection of fossils from the Trinil site, and chemical evidence associates them with the calotte (see below). Weidenreich considered

all of the Trinil femora to exhibit a basically similar morphology (although Femora II–V were more platymeric than Femur I), and to contrast in the same way with the Zhoukoudian femora (von Koenigswald and Weidenreich, 1939; Weidenreich, 1941).

Despite early objections, by the 1950s and 60s most researchers accepted the contemporaneity of the Trinil calotte and femora (Howells, 1959; Clark, 1964; Pilbeam, 1970), in part based on a fluorine analysis that indicated no significant differences between them (Bergman, 1952). Day and Molleson (1973) essentially duplicated the fluorine results, but on the basis of other analyses argued that they primarily demonstrated depositional rather than temporal similarities of the specimens. Later results of x-ray microanalyses showed Femur I to be distinct from the calotte and other Trinil femora, with Femur I being derived from an apparently more recent level (Day, 1986b; Bartsiokas and Day, 1993). Kennedy (1983: 587) carried out a detailed morphological study of *H. erectus* femora and concluded that the Trinil femora "showed a basically sapient pattern," although with some differences in the distal shaft (Kennedy's results are considered further in the Discussion). Based on these various reservations, later authors have generally taken a cautious approach to the Trinil femora, considering their association with the calotte and attribution to *H. erectus* to be uncertain (Aiello and Dean, 1990; Rightmire, 1990; Klein, 1999; Antón, 2003).

While the Trinil femora have been subjected to various morphological studies, to date no true structural analyses of biomechanically relevant parameters of these specimens have been carried out. Such analyses can give insights into body shape, posture, and behavior of past species (Lovejoy, 1979; Trinkaus et al., 1999; Ruff et al., 2006; Ruff, 2009; Puymerail et al., 2012), which in turn may also have taxonomic implications. In this study, using computed tomography (CT), we derive structural parameters of the femoral shafts of the five Trinil femora, and compare these to similar parameters measured on modern and Pleistocene *Homo* femora. We also compare CT Hounsfield numbers, related to physical density and composition (Hendee, 1983), between the Trinil femora, as a measure of relative fossilization of the specimens. Based on these analyses, we address the following questions: 1) How variable in structure and composition are the Trinil I–V femora? 2) How do Femora I–V compare structurally to other *Homo* femora, modern and earlier? 3) Do the Trinil femora conform to predictions of the early *Homo* "femoropelvic complex" (Day, 1984, 1986a; Ruff, 1995)?

Materials and methods

CT scanning and bone length estimates

The Trinil femora were CT scanned using a GE Lightspeed QX/I in the Rode Kruis Hospital, The Hague. Helical scanning mode was used, with a reconstructed slice thickness of 0.625 mm and a pixel size of 0.39 mm^2. As described in detail previously (Puymerail et al., 2012), a semi-automated threshold-based segmentation process was used to separate fossilized bone from any matrix. Endosteal contours were clearly visible at all levels. As noted by previous authors (Dubois, 1926, 1932, 1934; Day and Molleson, 1973), the external surfaces of the Trinil femora, especial II–V, are affected by varying degrees of weathering, abrasion, or damage (see Fig. 1). Small defects in the periosteal surface were filled in manually during image processing. Larger gaps, including missing cortex in the midshaft region of Femur III and mid-distal region of Femur IV (see Figs. 1 and 3), were not reconstructed.

Following previous studies (e.g., Ruff and Hayes, 1983; Trinkaus and Ruff, 1989; Puymerail et al., 2012), cross sections of the Trinil femora were analyzed at percentages of bone length' (biomechanical length), with length' defined as the distance parallel to the

Figure 2. Determination of femoral biomechanical neck length (heavy arrows) in Trinil Femur I and Femur II, measured mediolaterally from the most superior point on the head to the middle of the lateral surface of the greater trochanter. In Femur II, the dashed circle approximates the femoral head (see text); the solid outline is the reconstruction of the greater trochanter and superior femoral neck surface. Note that there is a 4% magnification between the scales, placed on the supporting surfaces, and measurements taken at the height of the head and greater trochanter.

long axis of the diaphysis between the average distal-most projection of the condyles and the superior surface of the neck (see also Ruff, 2002). For Femur I, this can be measured directly as 432 mm. For Femora II–V, following Antón et al. (2007) and Fellmann (2004), lengths were estimated using the general approach of Steele and McKern (1969), based on preserved anatomical landmarks. For Femora II–IV, the available preserved portions include Steele and McKern's Segment 2, the length parallel to the shaft between the center of the lesser trochanter and the point where the linea aspera begins to divide into the medial and lateral supracondylar lines. Proximal and distal landmarks of Segment 2 for Femora II–IV are illustrated in Supplementary Online Material (SOM) Figure 1, which shows local curvature maps of the posterior surfaces of the specimens derived from CT 3-D reconstructions. Landmarks were verified through personal inspection of the original specimens by one of us (CBR). Femur II preserves the (broken) outline of the lesser trochanter, and Femora III and IV are broken through the base of the lesser trochanter (SOM Fig. 1). All three specimens extend distally past the division of the linea aspera. Note that Day and Molleson's (1973: 135) assessment that the Trinil II femur "is broken just below the point where the linea aspera is beginning to divide" is somewhat misleading, since the beginning of the break occurs more than 50 mm distal to this point.

Linear regressions based on five different recent human samples were used to estimate maximum length from Segment 2 length (following Fellmann, 2004). The recent samples included Mississippian Native Americans (Steele and McKern, 1969), European-
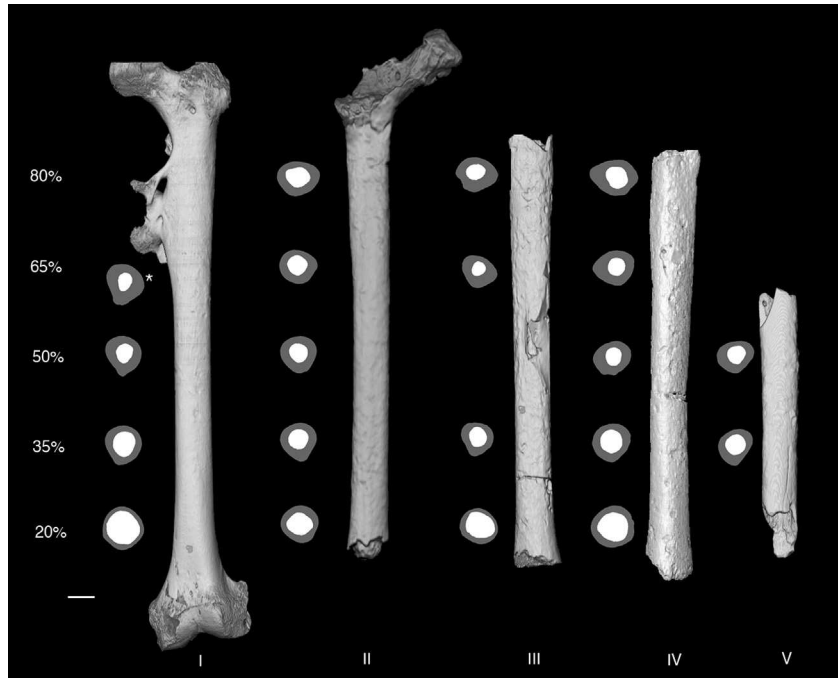
Figure 3. CT reconstructions of Trinil Femora I—V showing cross sections taken at 20%, 35%, 50%, 65%, and 80% of length' when available. Anterior is above and medial to the left in each image (images were reversed mediolaterally when necessary). Note that the 50% region for Femur III is missing a large section of the cortex, which we did not attempt to reconstruct. The 80% and 65% sections for Femur I are distorted by its exostosis; the undistorted 60% section (asterisk) is shown. The proximal portion of the head of Femur I was not included in the CT scans. Scale bar is 20 mm.

Americans and African-Americans (Steele, 1970), Alaskan Inuits (Fellmann, 2004), and Neolithic and Mesolithic Europeans (Jacobs, 1992). These are all of the available samples with such equations, although they do represent a diversity of body sizes and shapes, which may affect femoral proportions (e.g., see Ruff, 1995). Male and female equations from each sample were used, giving a total of 10 maximum length estimates, which were then averaged across all groups. Results are given in Table 1. Maximum length was then converted to length' using an equation based on 2053 femora from an on-going study of Upper Paleolithic through modern European skeletal samples (Ruff et al., 2012):

Femoral length' = Femoral maximum length * 0.9836 + 0.8 (r = 0.986, SEE = 4.6 mm).

Note that there are no equations for directly converting Segment 2 lengths to length' values.

Using this equation, femoral length' estimates for Femora II, III, and IV are 411 mm, 408 mm, and 406 mm, respectively. Cross sections were extracted at 1% intervals of length' between 20% (distal) and 80% (proximal) of length'. Because none of the Trinil femora, except for Femur I, preserve the complete proximal end, the 80% section was considered to lie 1.5 cm distal to the distal edge of the lesser trochanter, based on comparisons with comparably-sized modern femora.

Femur V is the most fragmentary of the Trinil specimens. Based on its anatomy, it clearly derives from the mid-distal portion of the shaft (Fig. 1; see also Dubois, 1934). Based on morphological comparisons to Femora II—IV, we assigned it a length' of 411 mm, equivalent to that of Femur II. This is slightly shorter than a similar measurement taken on Dubois' (1934) reconstruction of the specimen. Using this length estimate and preserved anatomical features (e.g., the distal termination of the linea aspera about 3 cm proximal to the most distal complete cross section), cross sections between about 25% and 57% of length' are preserved. This also matches quite closely with Dubois' (1934) original estimate of its relative position.

Cross-sectional properties

Sections were aligned relative to A-P and M-L axes following Ruff (2002), using anatomical features such as position of the linea aspera to help align the more fragmentary specimens (see Fig. 2). Following previously described procedures (Bondioli et al., 2010; Puymerail et al., 2012), cross-sectional properties (areas, second moments of area, external breadths) were calculated on virtual images reconstructed from the CT scans. To identify the position of minimum mediolateral (M-L) breadth, LOWESS curves (Cleveland, 1979) were fit (using a smoothing window of 0.3) to each distribution of M-L breadth against percentage of bone length'. The procedure is demonstrated for Trinil Femora I and II in SOM Figure 2. In addition to the Trinil femora, continuous cross-sectional data at 1% intervals were available for a sample of 20 modern (Roman and 19th century French) femora (Puymerail et al., 2012); these were used in analyses of the position of minimum M-L breadth relative to length'.

Cross-sectional data at 15% intervals from 20% to 80% of bone length' were available for a large sample of Early through Late Pleistocene *Homo* femora, mainly obtained from the summary by Trinkaus and Ruff (2012) (Table 2). Following earlier analyses (Puymerail et al., 2012), for comparative purposes these were divided into five morpho-chronological samples: Early Pleistocene (EP, >780,000 BP), early Middle Pleistocene (EMP, 400,000—780,000 BP), late Middle Pleistocene (LMP, 126,000—400,000 BP), Neandertals (Nea), and Late Pleistocene modern humans (LPMH).

Femoral neck length

Femoral biomechanical neck length (Ruff, 1995) was measured from scaled photographs of Trinil Femora I and II as the medio-lateral distance between the most superior point on the femoral

Table 1
Maximum length estimates (mm) from Segment 2 lengths using technique of Steele and McKern (1969).

Specimen	Segment 2	Maximum length estimate										
		Mississippian[b]		Euroamerican[c]		Af.-American[d]		Inuit[e]		Mes./Neol.[f]		
	Length[a]	Male	Female	Male	Female	Male	Female	Male	Female	Male	Female	Mean[g]
Femur II	235	426	426	431	409	436	416	463	445	474	457	438
Femur III	232	424	424	429	406	433	414	461	442	471	455	436
Femur IV	228	422	421	425	402	430	411	458	439	468	451	433

[a] Distance, parallel to the shaft, between center of lesser trochanter and distal-most extent of linea aspera before dividing into medial and lateral supracondylar lines.
[b] Steele and McKern (1969), *n*: males: 72, females: 29.
[c] Steele (1970), *n*: males: 50, females: 50.
[d] Steele (1970), *n*: males: 50, females: 50.
[e] Fellmann (2004), *n*: males: 61, females: 56.
[f] Jacobs (1992), *n*: males: 33, females: 26.
[g] Note that true maximum length in at least Femur II was likely to be about 10 mm longer than this (see text).

head and the midpoint of the lateral contour of the greater trochanter, with the femur in anatomical position (Fig. 2). Photographic magnification of images (4%) was determined by comparing total specimen length measurements of the original specimens and the photographs. Biomechanical neck length in Femur I was measured directly from its scaled photo as 58 mm. Because Femur II does not preserve the distal end, a bicondylar angle of 9°—average for modern human femora (Ruff, 1995) and also about equal to that for Femur I—was used for this specimen. The bicondylar angles of two African early *Homo* femora—KNM-ER 1472 and 1481a—are similar at 12° and 10°, respectively (Ruff, 1995). Even moderate changes in this angle (±5°) have a negligible effect on the estimated neck length of Trinil Femur II (<0.5 mm).

A sphere of 45 mm in diameter centered on the preserved femoral head core of Femur II (Fig. 2) was used to locate the approximate position of the most superior point of the head. Approximation of femoral head diameter in Femur II was based on comparisons with early Pleistocene *Homo* femora as well as Femur I (which has an equivalent diameter). KNM-ER 1472, 1481a, and Dmanisi D4167, all shorter than Trinil Femur II (lengths' of 376 mm, 370 mm, and about 362 mm, respectively; see Table 4), have femoral head breadths or estimated breadths between 40 and 44 mm (Lordkipanidze et al., 2007 [and personal measurement from their Fig. 2]; Trinkaus and Ruff, 2012); KNM-WT 15000, with a length' of 402 mm (pers. measurement), only slightly shorter than that of Trinil Femur II, has a femoral head breadth of 44.9 mm (Ruff, 2007); and OH 28, with a longer estimated length' of 425 mm, has an estimated femoral head breadth of 47.8 mm (Trinkaus and Ruff, 2012). Slight changes in femoral head breadth have a very small or no effect on the measurement of femoral neck length, depending on the centering of the sphere. A modest amount of lateral

Table 2
Comparative Pleistocene *Homo* samples.

Section	Sample	Specimens
20%	EP	KNM-ER 737, 1472, 1481a, 1808mn
	EMP	Aïn Maarouf 1
	Nea.	Amud 1, Chapelle-aux-Saints 1, Feldhofer 1, Ferrassie 1, Fond-de-Forêt 1, Spy 2
	LPMH	Skhul 4, 6, Cro-Magnon 1, 4322, Dolní Věstonice 3, 13, 14, 16, Minatogawa 1, 3, 4, Mladeč 27, Ohalo 2, Paviland 1, Pavlov 1, Tianyuan 1
35%	EP	KNM-ER 736, 737, 803, 1472, 1481a, 1808mn, Kresna 11
	EMP	Aïn Maarouf 1, Gesher-B.-Y. 1, OH 28
	LMP	Broken Hill E690
	Nea.	Amud 1, Chapelle-aux-Saints 1, Feldhofer 1, Ferrassie 1, 2, Fond-de-Forêt 1, Spy 2, Tabun 1
	LPMH	Qafzeh 9, Skhul 4, 5, 6, 7, Cro-Magnon 1, 4322, 4328, Dolní Věstonice 3, 13, 14, 16, 40, Minatogawa 1, 3, 4, Mladeč 27, Nahal 'En-Gev 1, Ohalo 2, Paviland 1, Pavlov 1, Sunghir 1, 4
50%	EP	KNM-ER 736, 737, 803a, 1472, 1481a, 1808mn, BOU_VP_2/15, 19/63, Kresna 11
	EMP	Aïn Maarouf 1, Gesher-B.-Y. 1, OH 28, Zhoukoudian 1, 2, 4, 5, 6
	LMP	Berg Aukas 1, Broken Hill E690, E793, Castel di Guido 1, La Chaise-BD 5, Ehringsdorf 5, Mammolo 1, Tabun E1
	Nea.	Amud 1, Chapelle-aux-Saints 1, Feldhofer 1, Ferrassie 1, 2, Fond-de-Forêt 1, Palomas 96, Quina 5, Rochers-de-V. 1, Saint-Césaire 1, Shanidar 4, 5, 6, Spy 2, Tabun 1, 3
	LPMH	Qafzeh 3, 8, 9, Skhul 3, 4, 5, 6, 7, Arene Candide 1, Barma Grande 2, Cro-Magnon 1, 4322, 4324, Dolní Věstonice 3, 13, 14, 16, 35, Grotte-des-Enfants 4, Minatogawa 1, 2, 3, 4, Mladeč 27, Nahal 'En-Gev 1, Ohalo 2, Paglicci 25, Paviland 1, Pavlov 1, Rochette 2, Sunghir 1, 4, Veneri 1, 2, Willendorf 1, Zhoukoudian-UC 67, UC 68
65%	EP	KNM-ER 736, 737, 803a, 1472, 1481a, 1808mn, Kresna 11
	EMP	Thomas Quarry,[a] Aïn Maarouf 1, Gesher-B.-Y. 1, OH 28
	LMP	Broken Hill E690, Tabun E1
	Nea.	Amud 1, Feldhofer 1, Ferrassie 1, 2, Fond-de-Forêt 1, Krapina 257.32, 257.33, Palomas 52, 92, 96, Quina 38, Shanidar 6, Spy 2
	LPMH	Qafzeh 6, 8, 9, Skhul 4, 5, Cro-Magnon 1, 4322, 4324, Dolní Věstonice 3, 13, 14, 16, 41, Minatogawa 1, 3, 4, Mladeč 27, 28, Nahal 'En-Gev 1, Ohalo 2, Paviland, Pavlov 1, Sunghir 1, 4, Tianyuan 1, Willendorf 1
80%	EP	KNM-ER 736, 737, 803a, 1472, 1481a, 1808mn, Kresna 11
	EMP	Gesher-B.-Y. 1, OH 28
	LMP	Broken Hill E689, E690, E709, La Chaise-BD 5, Tabun E1
	Nea.	Amud 1, Chapelle-aux-Saints 1, Feldhofer 1, Ferrassie 1, 2, Krapina 213, 214, Saint-Césaire 1, Spy 2, Tabun 1
	LPMH	Qafzeh 8, 9, Skhul 4, 5, 6, 9, Arene Candide 1, Barma Grande 2, Cro-Magnon 1, 4322, Dolní Věstonice 3, 13, 14, 16, 35, Grotte-des-Enfants 4, Minatogawa 1, 2, 3, 4, Mladeč 27, 28, Nahal 'En-Gev 1, Ohalo 2, Paglicci 25, Paviland 1, Pavlov 1, Rochette 2, Sunghir 1, 4, Tianyuan 1, Veneri 1, 2

[a] Unpublished specimen (E. Trinkaus, pers. comm.).

Table 3
Cross-sectional geometric properties at 15% intervals of bone length' from the distal end for the Trinil femora.[a]

Specimen	Section	TA	CA	%CA	Ix	Iy	Ix/Iy	J	Zx	Zy	Zp	Imax	Imin
Femur I	20%	776	282	36.3	30,062	27,178	1.11	57,241	1833	1718	3552	30,114	27,110
	35%	633	375	59.3	28,682	25,028	1.15	53,711	1947	1817	3768	28,688	25,080
	50%	593	448	75.5	30,486	23,976	1.27	54,462	2006	1794	3814	30,820	23,625
Femur II	20%	578	319	22.5	22,746	20,006	1.14	42,752	1649	1455	3104	22,521	20,303
	35%	554	382	69.1	24,197	21,037	1.15	45,235	1708	1567	3279	24,169	21,034
	50%	559	406	72.7	23,622	22,891	1.03	46,513	1732	1691	3423	23,689	22,847
	65%	576	395	68.6	22,545	26,957	0.84	49,502	1728	1847	3582	27,213	22,307
	80%	587	389	66.3	19,807	30,452	0.65	50,259	1584	1969	3594	30,513	19,697
Femur III	20%	685	293	42.8	24,670	26,147	0.94	50,817	1691	1686	3378	27,087	23,681
	35%	551	363	65.8	22,546	21,045	1.07	43,591	1630	1579	3210	23,246	20,334
	65%	529	430	81.4	22,248	24,082	0.92	46,329	1723	1708	3430	27,416	18,903
	80%	563	408	72.5	20,291	31,123	0.65	51,414	1631	1970	3642	31,691	19,695
Femur IV	20%	650	331	50.8	24,690	26,719	0.92	51,409	1732	1809	3542	27,231	24,152
	35%	551	347	62.9	20,909	21,224	0.99	42,133	1540	1566	3106	23,527	18,633
	50%	521	393	75.6	18,916	26,237	0.75	44,153	1501	1810	3327	27,706	16,470
	65%	542	416	76.7	18,800	29,267	0.64	48,067	1510	1983	3533	29,526	18,543
	80%	586	409	69.8	18,551	37,622	0.49	56,173	1534	2285	3934	37,895	18,315
Femur V	35%	490	314	64.1	19,386	16,745	1.16	36,131	1442	1329	2774	22,916	13,232
	50%	491	349	70.9	15,008	22,289	0.67	37,297	1260	1570	2858	23,166	14,148

[a] Abbreviations: TA, CA: total and cortical areas (mm^2); %CA: (CA/TA)*100; Ix, Iy: second moments of area about x and y axes (A-P and M-L bending rigidities, respectively; mm^4); J: polar second moment of area (torsional and twice average bending rigidity, mm^4); Zx, Zy: section moduli about x and y axes (A-P and M-L bending strengths, respectively; mm^3); Zp: polar section modulus (torsional and twice average bending strength, mm^3); Imax, Imin: maximum and minimum second moments of area (bending rigidities, mm^4).

projection of the mostly missing greater trochanter of Femur II was assumed (Fig. 2). Day and Molleson (1973) noted some cracking of bone around the base of the trochanter that they felt exaggerated the degree of lateral projection of the preserved portion, but any such distortion appeared minor upon examination of the original.

Because Femur II does not preserve the femoral condyles, it is not possible to directly factor in the possible effect of femoral neck anteversion on femoral biomechanical neck length, which is measured in the true M-L anatomical plane (Ruff, 1995). The position of Femur II in the photograph used to measure neck length (Fig. 2) is the same as that in which it was CT scanned (see Fig. 3), which shows the linea aspera oriented in a typical anatomical position (see also SOM Figure 1 for a complete contour map of the posterior surface of Femur II in this position). Thus, there is no anatomical evidence that the femoral neck in Figure 2 is not oriented anatomically. However, the effects of typical degrees of anteversion on femoral biomechanical neck length are relatively minor in any event. Femoral anteversion averages about 12° in

modern humans (Elftman, 1945), as well as early *Homo* (10° in KNM-ER 1471 and 15° in KNM-ER 1481a; pers. measurement). It can be shown trigonometrically that anteversion values in this range would reduce femoral biomechanical neck length by only 1.5—3.4% relative to neck length measured in the plane of the head and neck, i.e., maximum neck length.

To place Trinil Femora I and II into context, femoral biomechanical neck length relative to length' is compared in these specimens and five other Early Pleistocene specimens, four of which have been attributed to early *Homo* (Ruff, 1995; Lordkipanidze et al., 2007), as well as a sample of modern humans from Pecos Pueblo, New Mexico and East Africa (Ruff, 1995). Data for the fossil specimens are shown in Table 3. The modern human samples were chosen because they represent extremes of body shape and femoral neck length/total length proportions among modern humans (Ruff, 1995). To quantify relative neck length, following earlier analyses (Organ and Ward, 2006; Ruff, 2009), a reduced major axis regression line was fit through the modern human sample, and the deviations of the fossil data points from this line relative to the standard error of estimate of the line were calculated.

CT numbers

CT numbers, expressed in Hounsfield units, were used to investigate relative density, and by implication relative fossilization, of the Trinil specimens. CT numbers are related to both material density and chemical composition of the scanned material and can vary depending on a number of factors (Zatz, 1981; Hendee, 1983). By convention, air is assigned a value of −1000H and water a value of 0H. Modern long bone compact cortical bone typically has values in the range of about 1300—2300H (Ruff and Leo, 1986; Lam et al., 1998) and fossilized compact cortical bone may range up to values of 3000H or more (measured using standard medical CT systems; Spoor et al., 1993; Mafart et al., 2004). The H values for individual pixels within mediolateral cross-sectional traces at

Table 4
Femoral biomechanical neck length relative to femoral length' in Trinil Femora I and II, and five Early Pleistocene femora, compared to Pecos and East African modern humans.

Specimen[a]	Length' (mm)	Biom. Nk. Ln. (mm)	Rel. Dev.[b]
Trinil I	432	58	−0.22
Trinil II	411	72	2.59
KNM-ER 1472	376	59	1.70
KNM-ER 1481a	370	64	2.65
KNM-ER 3728	365	63	2.66
KNM-WT 15,000	402	69	2.41
Dmanisi D4167	362	67	3.37
Mean, modern sample	401	53	—

[a] Trinil I and II: present study; KNM-ER specimens: Ruff, 1995; KNM-WT 15000: pers. meas.; Dmanisi specimen measured from Figure 2 in Lordkipanidze et al. (2007).

[b] Fossil residual/modern sample standard error of estimate, based on reduced major axis regression through modern sample (see Fig. 6).

midshaft (50% sections) of the Trinil femora were determined from CT reconstruction matrices, and the distribution of values were compared between specimens.

Results

Available cross-sectional contours at 20%, 35%, 50%, 65%, and 80% of bone length' from the distal end for the five Trinil femora are shown in Figure 3. All sections are available in Femora II and IV; the 65% and 80% sections are distorted in Femur I because of the large proximal exostosis and were therefore not measured; the 50% section is unmeasurable in Femur III because of a large cortical defect in that region; and only the 35% and 50% sections are available in Femur V. A complete listing of structural properties at these locations is given in Table 3. The section contours at 60% of bone length for Femur I, the most proximal section not directly affected by the exostosis, are also shown in Figure 3.

Because none of the Trinil femora, except Femur I, preserve the femoral head, it is not possible to standardize cross-sectional properties by estimates of body size (e.g., Ruff et al., 2006; Trinkaus and Ruff, 2012). Instead, we concentrate our geometric analyses on critical shape characteristics that have been used to distinguish early *Homo* femora from those of more recent humans: the ratio of A-P (anteroposterior) to M-L bending rigidity at different locations on the shaft, the relative position of minimum M-L breadth of the shaft, and the relative length of the femoral neck (Weidenreich, 1941; Day, 1971; Kennedy, 1983; Ruff, 1995; Puymerail et al., 2012; Trinkaus and Ruff, 2012).

Figure 4 is a box plot of A-P/M-L bending rigidity at the five standard locations on the femoral shaft in the Trinil femora and five morpho-chronological samples of Pleistocene *Homo*. The ratio for the 60% section in Femur I is also plotted for reference with the 65% data. The ratio always increases between the 65% and 50% sections, so the position of this point is slightly too high, but is still likely close to what the true (undistorted) value for the Femur I 65% section would have been. As noted previously (Ruff, 1995;

Puymerail et al., 2012; Trinkaus and Ruff, 2012), Early and early Middle Pleistocene *Homo* femora have relatively increased mediolateral bending rigidity (lower A-P/M-L ratios) throughout the proximal and middle regions of the shaft compared to those of more recent *Homo*. Trinil Femora IV and V clearly show this pattern. Femora II and III also have low ratios in the most proximal (80%) section, although there is some overlap with more recent samples. Femur I has much higher ratios than the other Trinil femora in its most proximal (50% and 60%) sections, being most similar to Late Pleistocene modern humans. Interestingly, all of the Trinil femora tend to have somewhat high ratios in the distal two sections, especially the 20% location, consistent with Dubois' observation of a "convex" popliteal surface (Dubois, 1926, 1932; see also Fig. 3).

External mediolateral breadths at 1% intervals between 20% and 80% of length' are shown for the Trinil femora and a modern human sample (Roman and 19th century French) in Figure 5. The positions of minimum M-L breadth are indicated for each fossil specimen, along with the median and interquartile range of positions for the modern sample. The location of minimum breadth in Trinil Femora II–V occurs between 34% and 44% of length', below the inter-quartile range of the modern human sample (46—60%). The location in Femur I is more proximal, at 50% of length'. Trinil Femur IV is missing cortex in the 39—47% locations. Its minimum breadth occurs in the first section distal to this (38%) but could be more proximal; however, given the general longitudinal trend of values in this specimen (Fig. 5), it is highly likely that this occurred more distally than 44% of length'. All of the Trinil femora show less of an increase in M-L breadth distal to the point of minimum M-L breadth than the modern sample. This is consistent with their rounder cross sections in this region (see Figs. 3 and 4).

Femoral biomechanical neck length is plotted relative to length' for Trinil Femora I and II, five Early Pleistocene femora, and a sample of modern humans of diverse body shape (Ruff, 1995) in Figure 6. The relative deviations of the fossil specimens from a reduced major axis line through the modern sample are shown in Table 4. All of the Early Pleistocene specimens have relatively very long femoral necks, falling outside the 95% prediction interval (>2 SEE) of modern humans, except for KNM-ER 1472 (1.7 SEE), whose neck is damaged and may be artificially shortened (Day et al., 1975; Wolpoff, 1978). The one modern human outlier that overlaps with the range of the Early Pleistocene specimens is highly unusual in other respects, converging in shaft morphology with *H. erectus* (Ruff, 1995). Trinil Femur II falls close in relative position to the Early Pleistocene specimens, four of which have been attributed to *H. erectus* (KNM-ER 3728 may be *H. erectus* but is too weathered for a definitive attribution [Ruff, 1995]). In contrast, Trinil Femur I falls very close to the predicted value for modern humans.

Linear traces of Hounsfield CT numbers taken transversely across 50% sections of the five Trinil femora are shown in Figure 7 (the 45% section of Femur III was used here because of damage to the 50% section). The traces include air surrounding the specimens and any matrix within the medullary cavities. The distributions of individual pixel values for Hounsfield numbers within the cortical areas of each specimen (determined through reference to the whole section) are shown in Figure 8, along with median values. The data are truncated at 3071H, the maximum value provided by the scanner. All five femora reach this value in at least a few pixels. However, the overall distribution of values varies substantially between specimens. The median value for Femur I is about 2400H, with many (>40%) values falling between 2100 and 2300H, i.e., within the range of modern unfossilized compact cortical bone (Ruff and Leo, 1986). In contrast, median values for the other four Trinil femora are all at about 2700H or higher, with very few values below 2400H. The high H values observable in Femur I are all near the edges of the specimen, particularly the periosteal surface
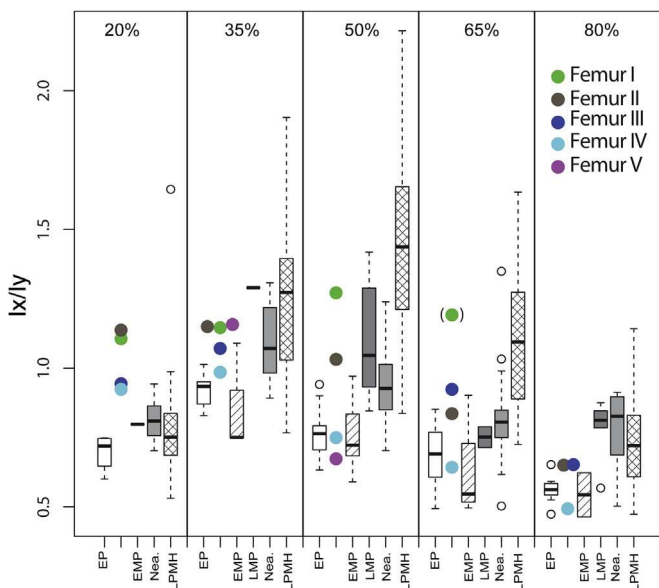

Figure 4. Ratios of A-P to M-L bending rigidity (Ix/Iy) in the Trinil femora relative to five morpho-chronological samples of Pleistocene *Homo* at five locations in the femoral shaft (80% is most proximal). EP: Early Pleistocene; EMP: early Middle Pleistocene; LMP: late Middle Pleistocene; Nea.: Neandertal; LPMH: Late Pleistocene modern humans. A-P/M-L bending rigidity of the 60% section for Trinil Femur I is shown in parentheses. For composition of the comparative samples, see Table 2.
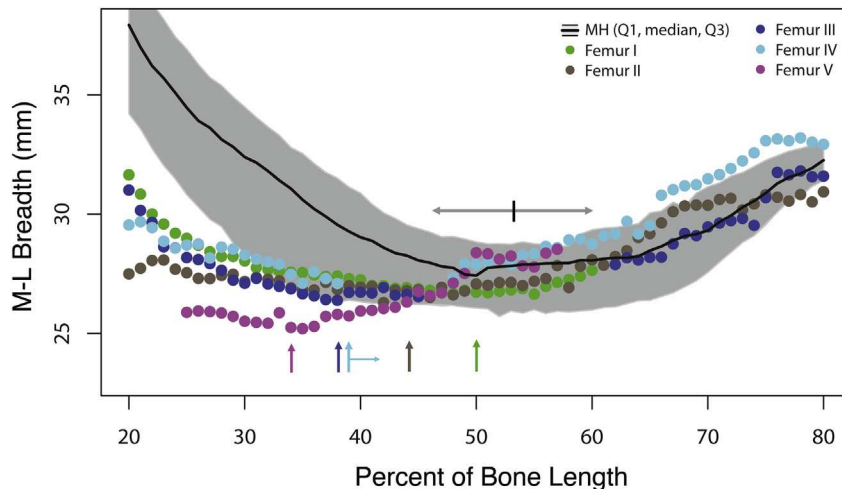
Figure 5. External mediolateral breadth of the Trinil femora and a sample of 20 modern human femora, sampled at 1% intervals of bone length'. The median (black line) and interquartile range (gray area) of absolute breadths at each location for the modern sample are plotted. Arrows for the Trinil specimens indicate positions of minimum M-L breadth, determined using LOWESS (see SOM Fig. 2). The true position of minimum breadth for Femur IV could be somewhat more proximal (see text). The black bar and gray arrows indicate the median ± interquartile range for the position of minimum M-L breath among the modern individuals.

(Fig. 7). Pixels in the interior of the cortex, more than a few millimeters from the external and internal surfaces, exhibit uniformly lower values (<2400H). Most of the other Trinil femora also show some decline in values in the middle of the cortex, but not to the same degree as in Femur I. To some extent this reduction of values in the interior of the cortices may reflect beam hardening (Hendee, 1983; Ruff and Leo, 1986), although this is unlikely to account for all of the reduction and does not explain the different patterns seen in

Femur I and the other femora. Note that the degree of filling of the medullary cavity with high density matrix varies greatly between specimens, with very little (at this section location) in Femora II and III, and almost complete filling in Femora I and IV.

Discussion

Weidenreich (1938, 1941) and Day (1971) described several features of Early/Middle Pleistocene *Homo* femora that taken together distinguished them from those of modern humans. Most of these features can be explained as adaptations to increase relative M-L bending rigidity or strength of the shaft, especially proximally (Ruff, 1995). This is directly reflected in A-P/M-L bending rigidity or strength proportions, and indirectly reflected in a low position of minimum M-L breadth, which results from expanded M-L dimensions more proximally. In both respects Trinil Femora II–V more closely group with Early/Middle Pleistocene *Homo* femora than does Trinil Femur I, which is similar to modern (i.e.,
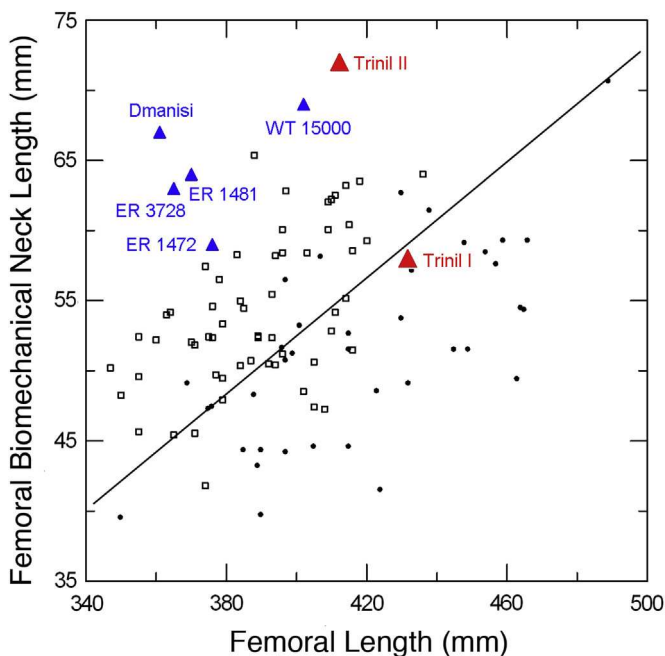

Figure 6. Femoral biomechanical neck length relative to femoral length' in modern humans (Pecos Puebloans, open squares; East Africans, filled circles), five Early Pleistocene femora (blue smaller triangles), and Trinil Femora I and II (red larger triangles). Modified from Ruff, 1995: Fig. 3. "ER" refers to KNM-ER, and "WT" to KNM-WT. "Dmanisi" is the D4167 specimen, measured from Figure 2 in Lordkipanidze et al. (2007). Reduced major axis regression line fit through combined modern human sample: Biom. Nk. Ln. = 0.205(Length') − 29.1.
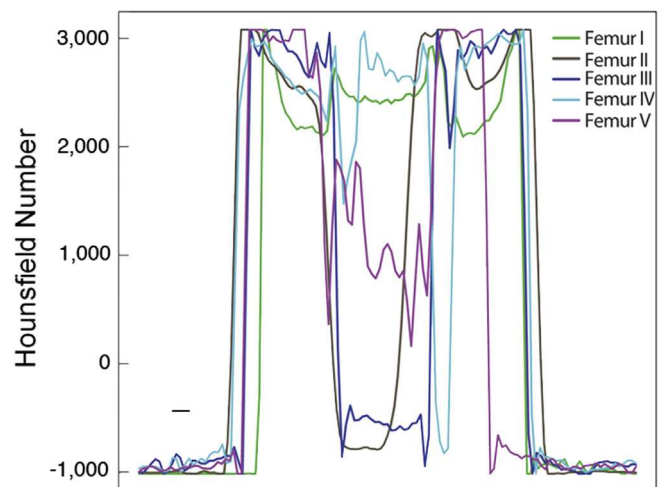

Figure 7. Mediolateral traces of Hounsfield numbers in CT sections through the Trinil femora, taken at 50% of length' (except in Femur III, taken at 45%), including both air external to the section and matrix within it, if present. Scale bar is 2 mm.
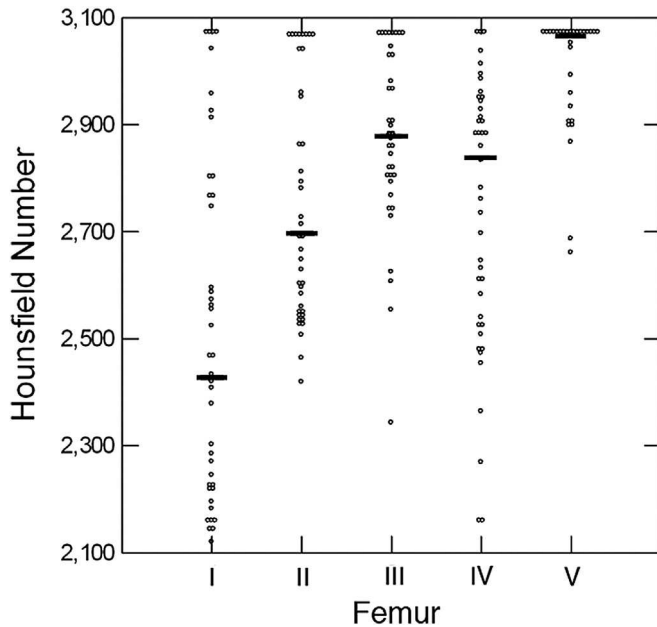
Figure 8. Hounsfield values of individual pixels for the cortical bone regions of each section shown in Fig. 7. Horizontal bars are median values. Note truncation of values at 3071H.

Late Pleistocene or Holocene) femora. The mediolateral strengthening of the proximal femoral shaft in early *Homo* can be attributed to a relatively long femoral neck, which increases M-L bending loads in the shaft (Ruff, 1995). This in turn may be related to a wide biacetabular breadth and several other associated features of the pelvis, part of the early *Homo* "femoropelvic complex" (Day, 1984, 1986a; Ruff, 1995). Restructuring of the pelvis in later *Homo*, and consequent changes in femoral morphology, may coincide with increases in relative cranial capacity and/or an altered birth mechanism (Ruff, 1995).

Trinil Femur II has a relatively long neck (in the same range as other early *Homo* femora), while Femur I is completely modern in this respect. Both the length of the femoral neck and total bone length are reconstructed in Femur II and subject to error. However, given the fairly conservative reconstruction of the position of the femoral head (Fig. 2), biomechanical neck length is unlikely to have been much shorter than its reconstructed value of 72 mm. Factoring in possibly (although unlikely) unaccounted for moderate anteversion would reduce its neck length by only about 1–2 mm. Increasing its length' by 20 mm (leading to an estimated maximum length of about 469 mm, almost a cm longer than Day's (1971) estimate) would still place it at about the upper 95% prediction interval for modern humans.

Day and Molleson felt that the large proximal exostosis in Trinil Femur I (see Fig. 1) had produced "distortion of the shaft" and that "its effects can be traced well down the shaft in the form of an unduly pronounced and deformed linea aspera that may well have affected the form of the shaft cross-section" (1973: 133). However, the nonpathological mid-diaphyseal (35%, 50%, and 60%) cross sections of Femur I are very typical in morphology for Holocene or Late Pleistocene early anatomically modern human femora, with no exaggeration of the linea aspera (e.g., see Ruff, 1995: Fig. 18; Trinkaus and Ruff, 1999: Fig. 3; Trinkaus, 2006: Figs. 18.15 and 18.16). The exostosis itself has been variously attributed to an injury (Dubois, 1894), an infection (Virchow, 1895), myositis ossificans (Day and Molleson, 1973), or fluorosis (Soriano, 1970), although this last diagnosis has been strongly questioned (Day and Molleson,

1973). Some minor arthritic changes in the distal femoral articular surface may be indirectly related to the more proximal lesion (Day and Molleson, 1973), but there is no indication that the morphology of the shaft itself, distal to the lesion, was significantly affected. In addition to the normal (for modern humans) general contours, there is no evidence for reduction of weight-bearing on that side, such as cortical thinning (Fig. 2) or a reduction in percent cortical area (Table 3). We also saw no evidence for "irregular opacification and uneven borders" of the cortex distal to the lesion (Kennedy, 1983: 607), unless this referred to the increased density of the outer cortex or high density matrix that fills most of the medullary cavity (Fig. 7).

The increased circularity of the distal shaft in all of the Trinil femora relative to modern humans is interesting, and consistent with Dubois' original observations (1926, 1932). This is also evident in some Early Pleistocene *Homo* femora, such as KNM-ER 1481a (Ruff, 1995: Fig. 18). It is possible that this is related to increased A-P loading about the knee joint, associated with high mobility (Ruff, 1987), which is not a trait diagnostic for early *Homo* alone.

Day (1971; see also Day and Molleson, 1973) and Kennedy (1983) assessed external (subperiosteal) and radiographically determined cortical breadths of the Trinil femora and concluded that in most respects they were not distinguishable from each other or from modern humans. Kennedy (1983: 613) noted that Trinil Femora II–IV shared relatively thick cortices with a group of *H. erectus* specimens, particularly in the mid-distal region of the shaft, but still concluded that "their overall morphological pattern clearly allies them with the sapiens." This was based in part on external shaft shape (A-P/M-L) indices determined at intervals along the diaphysis—when these were compared to those of modern human and *H. erectus* samples, the Trinil specimens fell closer to modern humans in the mid-proximal shaft (Kennedy, 1983: Fig. 2; also reproduced in Aiello and Dean, 1990: Fig. 21.27). However, there are some problems regarding the locations of some of the sections; for example, the "mid-shaft" section was taken "at the level of maximum A-P shaft diameter," which may bias its placement since it relies on shaft shape. The two most distal section locations were based on percentages of bone length. For these, Weidenreich's (1941) very long length estimate of 500 mm was used for Femur II, and Femur III was considered to be of equivalent length. Use of very long length estimates for incomplete specimens will obviously affect positioning of analogous section locations, and thus morphological comparisons. In addition, perhaps most importantly when interpreting any such results, external breadth indices are not equivalent to ratios calculated using true mechanical section properties (Stock and Shaw, 2007).

Weidenreich (1941) did not detail how he arrived at his estimate of about 500 mm for the length of Trinil Femur II, a figure that has been used not only in Kennedy's (1983) analyses but also in some later analyses of stature in *H. erectus* (Feldesman et al., 1990). Using the Steele and McKern (1969) method, we arrive at an estimate of 438 mm. However, this is almost certainly an underestimate of true maximum length, since it does not factor in the relatively longer femoral neck apparent in Femur II compared to that of modern humans. Based on those comparisons, a modern femur with a length' of 411 mm (our estimate for Femur II) would have a predicted biomechanical (mediolateral) neck length of about 55 mm (see Fig. 3), rather than 72 mm, as estimated here for Femur II. With a neck-shaft angle of 121° in Femur II, the effect of shortening neck length by 17 mm would be to reduce maximum length by about 10 mm. Applying this correction, the adjusted maximum femoral length of Femur II is 448 mm. This is very similar to the estimate of 447 mm by Fellmann (2004) and Antón et al. (2007), derived using a similar technique. Without more complete material, it is not possible to know if this correction also applies to Femora III and IV,

but if they form a coherent morphological and taxonomic group, as argued here, then it is also likely that their maximum lengths were on the order of a cm longer than those estimated by the Steele and McKern (1969) method (Table 1). It is still appropriate to use the Steele and McKern method on these femora, however, since the main objective here was to estimate length' for positioning of cross sections, and the maximum length to length' conversion that we used is based on femora with a modern morphology, i.e., a shorter femoral neck.

Day (1971) estimated the maximum length of Trinil Femur II as 460 mm, only slightly longer than our estimate. Use of the much longer Weidenreich estimate has consequences in addition to its effect on cross-sectional shape indices. First, the position of minimum M-L shaft breadth relative to length will move proximally (as more non-preserved bone is added distally), which explains why both Weidenreich (1941) and Kennedy (1983) found minimum M-L breadth of Femur III to be at about midshaft, rather than distal to midshaft, as found here (Fig. 5). Second, the proportion of neck length to shaft length will decrease, and this partly explains why Kennedy (1983) found essentially no difference between Trinil I and II in this characteristic (her estimate of femoral neck length in Trinil II also seems to be in error, as it is given as slightly shorter than that of Trinil I, which appears impossible based on the preserved morphology; see Fig. 2). As discussed above, even using a somewhat longer total bone length estimate, Femur II has a relatively very long neck. Use of a much longer length estimate for Femur II, or for any of the other incomplete Trinil femora, also affects assessments of the relative slenderness or gracility of the specimens (Weidenreich, 1941; Kennedy, 1983).

In addition to morphology, relative density, as inferred from CT Hounsfield numbers, distinguishes Trinil Femur I from the other Trinil femora. Femur I shows a pattern of density variation consistent with relatively more recent (i.e., incomplete) fossilization, whereby only the outermost cortex appears significantly more dense than modern unfossilized cortical bone. Femora II–V appear overall more fossilized, and the reduction in density in the interior cortex is less marked. (Some of the apparent reduction in density in the interior regions in all specimens is also likely due to beam hardening.) While the precise depositional environment of the different specimens would also have affected the process of fossilization, the results are at least consistent with a longer time period of fossilization of the latter group. As also pointed out by Day and Molleson (1973), most of the specimens, including Femur I, are filled with high density matrix to some degree. This, and the external fossilization of Femur I, explains the superficial similarity in appearance and "weight" of all of the femora (Fig. 1 and pers. obs.). As noted earlier, Femur I is also remarkable in showing very little surface weathering in comparison to the other Trinil femora; it is also much more complete. The present observations support other evidence (Day, 1986b; Bartsiokas and Day, 1993) that Femur I is derived from a different, more recent level than Femora II–V, consistent with its more modern morphology.

A very recent paper (Joordens et al., 2014), which appeared as the present paper was in press, included a discussion of the provenience of Femur I and concluded that there was no evidence that it derived from a more recent level at Trinil than the calotte (or, by implication, the other Trinil femora). We strongly disagree with this conclusion, for several reasons. First, the repeated assertion that Femur I is "heavily mineralized" (Joordens et al., 2014, Supplementary Information, pp. 5 and 11) is based on a superficial assessment of its external appearance and overall weight. As we show here (see above), only the outer few millimeters of the cortex of Femur I (and the cortex immediately adjacent to the endosteal border) have CT values above the range of modern unfossilized cortical bone. The similarity in external appearance of Femur I with

the other Trinil specimens (e.g., its "dark chocolate-brown color" (Joordens et al., 2014; SI p. 11)) is due to this external mineralization. The filling of the medullary cavity of Femur I with high density matrix (also noted by Day and Molleson, 1973: Plates 4 and 5) produces the impression that the bone is heavily fossilized, but our analysis shows that this is based on incomplete information and incorrect.

The large difference in composition between the outermost and more interior regions of the Femur I cortex that we demonstrate here may also explain the difference in results that Joordens et al. (2014) and Bartsiokas and Day (1993) obtained in their analyses of elemental composition of the Trinil specimens. As Joordens et al. note, their technique measured only the surface bone material of the specimens. Using this technique, Femur I is similar to the Trinil calotte and Femora II-V (Joordens et al., 2014: Table S3). However, using material obtained from deeper in the cortex, Bartsiokas and Day (1993) found significant differences between Femur I and all of the other Trinil specimens. While the precise causal relationship between our CT values and the elemental data obtained by Joordens et al. and Bartsiokas and Day cannot be determined without more information, the similarity in results between the three studies (Femur I bearing a literally superficial but not deeper resemblance to the other Trinil specimens) supports our contention that the depositional history of Femur I was different from that of the other specimens.

Joordens et al. (2014) also rely heavily on Kennedy's (1983) visual assessment of radiographs of Femur I, in which she described "irregular opacification" and other purportedly pathological features distal to the exostosis. This is used to argue both against employing morphology to evaluate Femur I's taxonomic status, as well as to explain the difference in results obtained by Bartsiokas and Day (1993). However, Kennedy (1983) provided no evidence in support of these visual observations. Day and Molleson (1973), who also took radiographs of the Trinil specimens, do not mention these features. In fact, they note that "microradiographs made of thin sections cut from the cortex of Femur I confirmed the normal nature of the bone" (p. 143). We saw no evidence for "irregular opacification" of the cortical bone of Femur I distal to the exostosis (e.g., see Fig. 7). The "presence of linear areas of vertically oriented increased density along the cortico-medullary boundary, extending the entire length of the shaft" noted by Kennedy (1983: 607) and cited by Joordens et al. (2014: SI p. 8), may have been her impression based on the increased density of the Femur I cortex adjacent to the matrix-filled medullary cavity (Fig. 7), or even the matrix itself. However, there is no evidence that the bone itself exhibits pathological alteration distal to the exostosis. As noted above, the cross-sectional geometry of sections taken distal to the exostosis is completely normal in appearance (for a Late Pleistocene or Holocene anatomically modern human), with no unusual or irregular cortical thickening or thinning, exaggeration of the linea aspera, etc. that might reflect a pathological process (Fig. 3). There is thus no valid reason for excluding consideration of shaft morphology in taxonomic assessments of Femur I. One other factor that can be noted in this regard: relative femoral neck length, which also strongly allies Femur I with modern humans and not early *Homo* (Fig. 6), is extremely unlikely to have been affected by any later pathological process affecting the shaft region. Thus, *contra* Joordens et al. (2014), both the morphology and composition of Femur I argue against its association with the other Trinil femora, or inclusion within *Homo erectus*.

Conclusions

Trinil Femur I does not exhibit any of the structural features that have been found to characterize early *Homo* femora in other

regions, i.e., a relatively long neck, increased mediolateral bending rigidity of the mid-proximal shaft, or a distal position of minimum M-L breadth of the shaft, compared to modern humans. Where these features can be evaluated, the morphology of Trinil Femora II–V is more consistent with the early *Homo* pattern. They also appear to be more heavily fossilized than Femur I. Thus, with respect to both structure and composition, the two groups are distinct, with Femora II–V more closely fulfilling expectations based on the early *Homo* "femoropelvic complex" (Day, 1984, 1986a; Ruff, 1995), as well as a longer period of deposition. It is not possible to say from our results whether any of the femoral specimens is more closely associated (temporally) with the Trinil calotte, although other chemical evidence groups the calotte more closely with Femora II–V than with Femur I (Day, 1986b; Bartsiokas and Day, 1993). On morphological grounds, Femur I would fit comfortably within Late Pleistocene modern *Homo sapiens*, while Femora II–V would not. Thus, long-held doubts expressed about the contemporaneity of the calotte and Femur I are supported by our results. This is somewhat ironic given that the morphology of Femur I inspired the species attribution of "erectus" to both the calotte and femur. However, Trinil Femora II–V do support the possible presence of typical early *Homo* postcranial morphology at Trinil, which would be consistent with evidence from the calotte.

Acknowledgments

Appendix A. Supplementary data

Supplementary data related to this article can be found at http://dx.doi.org/10.1016/j.jhevol.2014.12.004.

References

Aiello, L., Dean, C., 1990. An Introduction to Human Evolutionary Anatomy. Academic Press, London.

Antón, S.C., 2003. Natural history of *Homo erectus*. Am. J. Phys. Anthropol. (Suppl. 37), 126–170.

Antón, S.C., Spoor, F., Fellmann, C.D., Swisher, C.C., 2007. Defining *Homo erectus*: size considered. In: Henke, W., Tattersall, I., Hardt, T. (Eds.), Handbook of Paleoanthropology, Vol. 3. Springer-Verlag, Berlin, pp. 1655–1693.

Barstra, G.-J., 1982. The river-laid strata near Trinil, site of *Homo erectus*, Java, Indonesia. Mod. Quart. Res. S.E. Asia 7, 97–130.

Bartsiokas, A., Day, M.H., 1993. Electron-probe energy-dispersive x-ray-microanalysis (edxa) in the investigation of fossil bone − the case of Java Man. Proc. R. Soc. Lond. Series B 252, 115–123.

Bergman, R.A.M., 1952. The fluorine content of *Pithecanthropus* and of other specimens from the Trinil fauna. Proc. Koninklijke Nederlandse Akademie van Wetenschappen, Series B 55, 150–152.

Bondioli, L., Bayle, P., Dean, C., Mazurier, A., Puymerail, L., Ruff, C., Stock, J.T., Volpato, V., Zanolli, C., Macchiarelli, R., 2010. Technical note: Morphometric maps of long bone shafts and dental roots for imaging topographic thickness variation. Am. J. Phys. Anthropol. 142, 328–334.

Buxton, L.H.D., 1938. Platymeria and platycnemia. J. Anat. 73, 31–36.

Clark, W.E.L.G., 1939. The relationship between *Pithecanthropus* and *Sinanthropus*. Nature 145, 70–71.

Clark, W.E.L.G., 1964. The Fossil Evidence for Human Evolution, 2nd ed. University Chicago Press, Chicago.

Cleveland, W.S., 1979. Robust locally weighted regression and smoothing scatterplots. J. Am. Stat. Assoc. 74, 829–836.

Cunningham, D.J., 1895. Dr. Dubois' so-called missing link. Nature 51, 428–429.

Day, M.H., 1971. Postcranial remains of *Homo erectus* from Bed IV, Olduvai Gorge, Tanzania. Nature 232, 383–387.

Day, M.H., 1984. The postcranial remains of *Homo erectus* from Africa, Asia, and possibly Europe. Cour. Foresch. Inst. Senckenberg 69, pp. 113–121.

Day, M.H., 1986a. Bipedalism: Pressures, origins and modes. In: Wood, B., Martin, L., Andrews, P. (Eds.), Major Topics in Primate and Human Evolution. Cambridge University Press, Cambridge, pp. 188–202.

Day, M.H., 1986b. *Homo erectus*: an old species with new problems. Bull. Soc. R. Belge Anthropol. Prehist. 97, 33–44.

Day, M.H., Molleson, T.I., 1973. The Trinil femora. In: Day, M. (Ed.), Human Evolution. Symp. S.S.H.B., Vol. 11. Taylor and Francis, London, pp. 127–154.

Day, M.H., Leakey, R.E.F., Walker, A.C., Wood, B.A., 1975. New hominids from East Rudolf, Kenya, I. Am. J. Phys. Anthropol. 42, 461–476.

de Vos, J., 2008. Receiving an ancestor in the phylogenetic tree. J. Hist. Biol. 42, 361–379.

Dubois, E., 1893. Palaeontologische onderzoekingen op Java. Verslag van het Mijnwezen Third Quarter 1892, p. 13; translated in: Meikle, W.E., Parker, S.T., 1994. In: Naming our Ancestors. An Anthology of Hominid Taxonomy. Waveland Press, Prospect Heights, Illinois, pp. 37–40.

Dubois, E., 1894. *Pithecanthropus erectus*, eine menschednahnliche Uebergangsform aus Java. National Press, Batavia.

Dubois, E., 1895. On *Pithecanthropus erectus* of the Pliocene of Java. Bull. Soc. Belge Geol. 9, 151–160.

Dubois, E., 1896. On *Pithecanthropus erectus*: a transitional form between man and the apes. J. Anthropol. Inst. Great Britain and Ireland 25, 240–255.

Dubois, E., 1926. On the principal characters of the femur of *Pithecanthropus erectus*. Proc. Koninklijke Nederlandse Akademie van Wetenschappen 29, 730–743.

Dubois, E., 1932. The distinct organization of *Pithecanthropus* of which the femur bears evidence, now confirmed from other individuals of the described species. Proc. Koninklijke Nederlandse Akademie van Wetenschappen 35, 716–722.

Dubois, E., 1934. New evidence of the distinct organization of *Pithecanthropus*. Proc. Koninklijke Nederlandse Akademie van Wetenschappen 37, 139–145.

Dubois, E., 1935. The sixth (fifth new) femur of *Pithecanthropus erectus*. Proc. Koninklijke Nederlandse Akademie van Wetenschappen 38, 850–852.

Elftman, H., 1945. Torsion of the lower extremity. Am. J. Phys. Anthropol. 3, 255–265.

Feldesman, M.R., Kleckner, J.G., Lundy, J.K., 1990. The femur/stature ratio and estimates of stature in mid- and late-Pleistocene fossil hominids. Am. J. Phys. Anthropol. 83, 359–372.

Fellmann, C.D., 2004. Estimation of femoral length and stature in fossil and modern hominins: a test of methods. MA thesis, Rutgers University.

Gilbert, W.H., 2008. Daka member hominid postcranial remains. In: Gilbert, W.H., Asfaw, B. (Eds.), *Homo erectus*: Pleistocene Evidence from the Middle Awash, Ethiopia. University California Press, Berkeley, pp. 373–396.

Hendee, W.H., 1983. The Physical Principles of Computed Tomography. Little, Brown and Co., Boston.

Hepburn, D., 1896. The Trinil femur (*Pithecanthropus erectus*) contrasted with the femora of various savage and civilized races. J. Anat. Physiol. 11, 1–17.

Howells, W., 1959. Mankind in the Making. Doubleday and Co., New York.

Jacobs, K., 1992. Estimating femur and tibia length from fragmentary bones: an evaluation of Steele's (1970) method using a prehistoric European sample. Am. J. Phys. Anthropol. 89, 333–345.

Joordens, J.C., d'Errico, F., Wesselingh, F.P., Munro, S., de Vos, J., Wallinga, J., Ankjaergaard, C., Reimann, T., Wijbrans, J.R., Kuiper, K.F., Mucher, H.J., Coqueugniot, H., Prie, V., Joosten, I., van Os, B., Schulp, A.S., Panuel, M., van der Haas, V., Lustenhouwer, W., Reijmer, J.J., Roebroeks, W., 2014. *Homo erectus* at Trinil on Java used shells for tool production and engraving. Nature. http://dx.doi.org/10.1038/nature13962.

Kennedy, G.E., 1983. Some aspects of femoral morphology in *Homo erectus*. J. Hum. Evol. 12, 587–616.

Klein, R., 1999. The Human Career, 2nd ed. University of Chicago Press, Chicago.

Lam, Y.M., Chen, X.B., Marean, C.W., Frey, C.J., 1998. Bone density and long bone representation in archaeological faunas: comparing results from CT and photon densitometry. J. Archaeol. Sci. 25, 559–570.

Lordkipanidze, D., Jashashvili, T., Vekua, A., Ponce de Leon, M.S., Zollikofer, C.P., Rightmire, G.P., Pontzer, H., Ferring, R., Oms, O., Tappen, M., Bukhsianidze, M., Agusti, J., Kahlke, R., Kiladze, G., Martinez-Navarro, B., Mouskhelishvili, A., Nioradze, M., Rook, L., 2007. Postcranial evidence from early *Homo* from Dmanisi, Georgia. Nature 449, 305–310.

Lovejoy, C.O., 1979. Contemporary methodological approaches to individual primate fossil analysis. In: Morbeck, M.E., Preuschoft, H., Gomberg, N. (Eds.), Environment, Behavior and Morphology: Dynamic Interactions in Primates. Gustav Fischer, New York, pp. 229–243.

Mafart, B., Guipert, G., de Lumley, M.A., Subsol, G., 2004. Three-dimensional computer imaging of hominid fossils: a new step in human evolution studies. Canad. Assoc. Radiol. J. 55, 264–270.

Mayr, E., 1944. On the concepts and terminology of vertical subspecies and species. Natl. Res. Council Bull. (Documents of the Committee on Common Problems of Genetics, Paleontology, and Systematics) 2, 11–16.

Mayr, E., 1950. Taxonomic categories in fossil hominids. Cold Spring Harbor Symp. Quant. Biol. 15, 109–118.

Organ, J.M., Ward, C.V., 2006. Contours of the hominoid lateral tibial condyle with implications for *Australopithecus*. J. Hum. Evol. 51, 113–127.

Pearson, K., Bell, J., 1919. A Study of the Long Bones of the English Skeleton. Cambridge University Press, London.

Pilbeam, D.R., 1970. The Evolution of Man. Thames and Hudson, London.

Puymerail, L., Ruff, C.B., Bondioli, L., Widianto, H., Trinkaus, E., Macchiarelli, R., 2012. Structural analysis of the Kresna 11 *Homo erectus* femoral shaft (Sangiran, Java). J. Hum. Evol. 63, 741–749.

Rightmire, G., 1990. The Evolution of *Homo erectus*. Cambridge University Press, Cambridge.

Ruff, C.B., 1987. Sexual dimorphism in human lower limb bone structure: relationship to subsistence strategy and sexual division of labor. J. Hum. Evol. 16, 391–416.

Ruff, C.B., 1995. Biomechanics of the hip and birth in early *Homo*. Am. J. Phys. Anthropol. 98, 527–574.

Ruff, C.B., 2002. Long bone articular and diaphyseal structure in Old World monkeys and apes, I: locomotor effects. Am. J. Phys. Anthropol. 119, 305–342.

Ruff, C.B., 2007. Body size prediction from juvenile skeletal remains. Am. J. Phys. Anthropol. 133, 698–716.

Ruff, C.B., 2009. Relative limb strength and locomotion in *Homo habilis*. Am. J. Phys. Anthropol. 138, 90–100.

Ruff, C.B., Hayes, W.C., 1983. Cross-sectional geometry of Pecos Pueblo femora and tibiae – a biomechanical investigation. I. Method and general patterns of variation. Am. J. Phys. Anthropol. 60, 359–381.

Ruff, C.B., Leo, F.P., 1986. Use of computed tomography in skeletal structure research. Yrbk. Phys. Anthropol. 29, 181–195.

Ruff, C.B., Holt, B.M., Sladek, V., Berner, M., Murphy Jr., W.A., zur Nedden, D., Seidler, H., Recheis, W., 2006. Body size, body proportions, and mobility in the Tyrolean "Iceman". J. Hum. Evol. 51, 91–101.

Ruff, C.B., Holt, B.M., Niskanen, M., Sladek, V., Berner, M., Garofalo, E., Garvin, H.M., Hora, M., Maijanen, H., Niinimaki, S., Salo, K., Schuplerova, E., Tompkins, D., 2012. Stature and body mass estimation from skeletal remains in the European Holocene. Am. J. Phys. Anthropol. 148, 601–617.

Shipman, P., 2001. The Man Who Found the Missing Link: Eugene Dubois and his Lifelong Quest to Prove Darwin Right. Simon and Schuster, New York.

Soriano, M., 1970. The fluoric origin of the bone lesion in the *Pithecanthropus erectus* femur. Am. J. Phys. Anthropol. 32, 49–57.

Spoor, C.F., Zonneveld, F.W., Macho, G.A., 1993. Linear measurements of cortical bone and dental enamel by computed tomography: applications and problems. Am. J. Phys. Anthropol. 91, 469–484.

Steele, D.G., 1970. Estimation of stature from fragments of long limb bones. In: Stewart, T.D. (Ed.), Personal Identification in Mass Disasters. National Museum of Natural History, Smithsonian Institution, Washington, DC, pp. 85–97.

Steele, D.G., McKern, T.W., 1969. A method for assessment of maximum long bone length and living stature from fragmentary long bones. Am. J. Phys. Anthropol. 31, 215–227.

Stock, J.T., Shaw, C.N., 2007. Which measures of diaphyseal robusticity are robust? A comparison of external methods of quantifying the strength of long bone diaphyses to cross-sectional geometric properties. Am. J. Phys. Anthropol. 134, 412–423.

Theunissen, B., 1989. Eugene Dubois and the Ape-Man from Java. Kluwer, Dordrecht.

Trinkaus, E., 2006. The lower limb remains. In: Trinkaus, E., Svoboda, J. (Eds.), Early Modern Human Evolution in Central Europe. The People of Dolní Vestonice and Pavlov. Oxford University Press, Oxford, pp. 380–418.

Trinkaus, E., Ruff, C.B., 1989. Diaphyseal cross-sectional morphology and biomechanics of the Fond-de-Forêt 1 femur and the Spy 2 femur and tibia. Bull. Soc. R. Belge Anthropol. Préhist. 100, 33–42.

Trinkaus, E., Ruff, C.B., 1999. Diaphyseal cross-sectional geometry of Near Eastern Middle Paleolithic humans: the femur. J. Archaeol. Sci. 26, 409–424.

Trinkaus, E., Ruff, C.B., 2012. Femoral and tibial diaphyseal cross-sectional geometry in Pleistocene *Homo*. PaleoAnthropology 2012, 13–62.

Trinkaus, E., Stringer, C.B., Ruff, C.B., Hennessy, R.J., Roberts, M.B., Parfitt, S.A., 1999. Diaphyseal cross-sectional geometry of the Boxgrove 1 Middle Pleistocene human tibia. J. Hum. Evol. 37, 1–25.

Virchow, R., 1895. Die frage vondem *Pithecanthropus erectus*. Zeitschrift fur Ethnologie 27, 435–442.

von Koenigswald, G.H.R., Weidenreich, F., 1939. The relationship between *Pithecanthropus* and *Sinanthropus*. Nature 144, 926–929.

Weidenreich, F., 1938. The discovery of the femur and the humerus of *Sinanthropus pekinensis*. Nature 141, 614–617.

Weidenreich, F., 1941. The extremity bones of *Sinanthropus pekinensis*. Paleont. Sinica (N.S. D.) 5D, 1–150.

Wolpoff, M.H., 1978. Some implications of relative biomechanical neck length in hominid femora. Am. J. Phys. Anthropol. 48, 143–148.

Zatz, L.M., 1981. Basic principles of computed tomography scanning. In: Newton, T.H., Potts, D.G. (Eds.), Radiology of the Skull and Brain: Technical Aspects of Computed Tomography. C.V. Mosby, St. Louis, pp. 3853–3876.